Optical Force Enhancement Using an Imaginary Vector Potential for Photons

Lana Descheemaeker,[1] Vincent Ginis,[1,2,*] Sophie Viaene,[1,3] and Philippe Tassin[3,1]
[1]Applied Physics Research Group, Vrije Universiteit Brussel, Pleinlaan 2, B-1050 Brussel, Belgium
[2]Harvard John A. Paulson School of Engineering and Applied Sciences, Harvard University, Cambridge, Massachusetts 02138, USA
[3]Department of Physics, Chalmers University of Technology, SE-412 96 Göteborg, Sweden
(Received 8 February 2017; published 27 September 2017)

The enhancement of optical forces has enabled a variety of technological applications that rely on the optical control of small objects and devices. Unfortunately, optical forces are still too small for the convenient actuation of integrated switches and waveguide couplers. Here we show how the optical gradient force can be enhanced by an order of magnitude by making use of gauge materials inside two evanescently coupled waveguides. To this end, the gauge materials inside the cores should emulate imaginary vector potentials for photons pointing perpendicularly to the waveguide plane. Depending on the relative orientation of the vector potentials in neighboring waveguides, i.e., pointing away from or towards each other, the conventional attractive force due to an even mode profile may be enhanced, suppressed, or may even become repulsive. This and other new features indicate that the implementation of complex-valued vector potentials with non-Hermitian waveguide cores may further enhance our control over mode profiles and the associated optical forces.

DOI: 10.1103/PhysRevLett.119.137402

The exchange of momentum between electromagnetic waves and matter is a fascinating effect with a long scientific history [1]. For a long time, optical forces were considered to be too minute for "terrestrial affairs" [2]. Indeed, it took more than thirty years before the radiation pressure, theoretically predicted by Maxwell, was detected by Lebedew [3] and Nichols and Hull [4] in high-precision torsion experiments. Now, one century later, the manipulation and actuation of objects through the use of optical forces has become a thriving scientific and technological research field [5–12]. When sufficiently enhanced, optical forces can, e.g., be used to manipulate microscopic objects [13–18], to cool down atomic gasses and cavities [19,20], to sort molecules and cells [21–23], to probe mechanical quantum states [6], and to optically control motors, optical filters, and integrated switches [24–28].

The aforementioned applications have resulted from continuous research efforts to enhance optical forces through the engineering of light modes. This has been done using appropriately structured light sources [7,17,19], the individual or collective response of resonators [29–32], or structured interfaces and waveguides to confine modes [5,33–37]. A waveguide geometry is particularly well suited for the enhancement of optical forces [15,26,32,38–41]. Indeed, the optical gradient force depends on the amplitude and on the lateral decay length of the electric field, both of which can be enhanced in a waveguide setup [42]. Scientists have taken advantage of large gradient forces between waveguides to implement integrated switches and actuators [26,35,36,38]. In these devices, gradient forces with a magnitude of the order of several pN μm^{-1} mW^{-1} have been obtained [26,35,36]. Still, further enhancement is required for optical forces to be used in a convenient way in integrated optics.

In this Letter, we propose a new mechanism for the enhancement of optical forces that relies on the modification of the confined mode profile inside waveguides that implement complex-valued artificial effective gauges. In the past few years, researchers have successfully transposed the effects of a vector potential on charged particles [43–45] to charge-neutral particles and photons [46–55]. Similarly to the case of charged particles, an effective vector potential $\tilde{\mathbf{A}}$ shifts the pseudomomentum of photons to $\mathbf{k} - \tilde{\mathbf{A}}$. This shift was recently used to introduce a waveguide design [56] with new dispersion properties of light propagating parallel to the direction of the vector potential in a gauge material, and has been experimentally demonstrated last year [57,58]. Here, we demonstrate that the application of a complex-valued vector potential to a waveguide core, perpendicular to the propagation direction of guided modes, may enhance the optical force by an order of magnitude, both through an optimization of the mode profile and the appearance of gauge-dependent terms in the Lorentz force. Such an imaginary vector potential is generated by specific non-Hermitian materials such as coupled loss-gain resonators, as discussed in Ref. [59]. In the Supplemental Material [60] and Refs. [61,62] therein, we discuss how to implement these imaginary gauges in a waveguide geometry (see Fig. S4).

To obtain some physical intuition into the significance and implementation of complex-valued vector potentials, we first revisit the well-known case of real vector potentials. In the presence of a real vector potential $\tilde{\mathbf{A}}$, a photon accumulates a nontrivial phase $\Phi = \int \tilde{\mathbf{A}} \cdot d\mathbf{l}$ along its

trajectory [49,63]. The implementation of this phase, by making use of coupled resonators and waveguides, has enabled the experimental demonstration of effective magnetic fields, robust transport of light, and optical isolators [53,63,64]. In the case of an imaginary vector potential, a photon accumulates an imaginary phase along a trajectory [59]. Therefore, imaginary vector potentials reduce or increase the photon's amplitude depending on the direction in which they travel. As a result, the implementation of imaginary vector potentials requires the use of non-Hermitian systems such as loss-gain waveguides or resonators [59,61,62,65] (Fig. S4 in the Supplemental Material [60]).

To enhance the optical force between a pair of slab waveguides with cores of thickness a and refractive index n_{core} larger than the vacuum cladding regions, we apply an imaginary gauge potential perpendicular to the waveguides. As shown in Fig. 1, we only consider symmetric orientations of the imaginary gauges; i.e., the gauge in the rightmost waveguide ($\tilde{\mathbf{A}} = i\,\tilde{A}\,\mathbf{1}_x$) is the mirror image of the leftmost waveguide. Following the methodology developed in Ref. [56], our description of effective gauge potentials inside the waveguides relies on minimal substitution in the Maxwell equations, replacing partial derivatives ∇ by covariant derivatives $\nabla - i\tilde{\mathbf{A}}$. As a result of minimal substitution, effective gauges may modify the dispersion and/or the mode profile of guided waves based on their contributions to the wave equation in the core region.

The electric fields of transverse-electric guided modes in a single-slab gauge waveguide, i.e., $\mathbf{E} = \phi(x)\exp[i(\beta z - \omega t)]\mathbf{1}_y$, consist of a remarkable mode profile $\phi(x)$ propagating along the z direction with wave vector β and oscillating at frequency ω. Inside the core, the electric field is a solution to the following wave equation, which has been derived from the Maxwell equations through minimal substitution:

$$\frac{\partial^2\phi(x)}{\partial x^2} + 2\tilde{A}\frac{\partial\phi(x)}{\partial x} - \left[\beta^2 - \tilde{A}^2 - \left(\frac{\omega n}{c}\right)^2\right]\phi(x) = 0. \quad (1)$$

In general, the solutions to this wave equation are damped harmonic functions, where the damping is directly proportional to the strength of the gauge field $\tilde{A}$. Because of the continuity of electric and magnetic fields at the edges of the waveguide, only the underdamped mode profiles can lead to nontrivial guided modes. Defining a normalization constant C_{core}, we can write the transverse electric field of a mode inside the core as

$$\phi(x) = C_{\text{core}} e^{-Ax}\cos(kx + \varphi). \quad (2)$$

As shown in Fig. 1(a), the oscillating mode profile is no longer symmetric, but is now enclosed by an exponential envelope that depends on the gauge field $\tilde{\mathbf{A}}$ inside the core. Outside of the core, the electromagnetic fields decay exponentially to ensure confinement. The corresponding

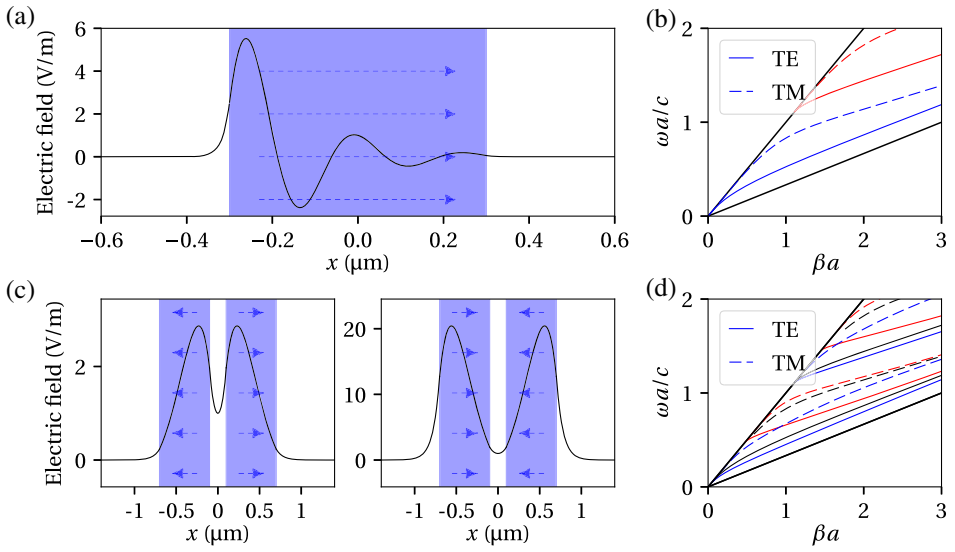

FIG. 1. Comparison of the mode profiles and dispersion relations of single-slab waveguides (a)–(b) and two coupled slab waveguides (c)–(d), where the core refractive index is higher than that of the cladding and an imaginary gauge vector potential is applied in the direction of the arrows. (a) The mode profile is exponentially damped inside the core of a waveguide with an imaginary vector potential perpendicular to the propagation direction. (b) The dispersion relation is unchanged with respect to a conventional slab waveguide and contains even (blue) and odd (red) modes with TE (full line) and TM (dashed line) polarizations. (c) Coupled waveguides with imaginary gauges. Gauges that point away from (towards) each other lead to attractive (repulsive) forces. (d) The dispersion relation of two coupled waveguides corresponds to hybridized modes of a single-slab waveguide (black), and does not depend on the magnitude of the gauge potential.

magnetic fields are easily found through the application of Faraday's law in the presence of a vector potential (applying minimal substitution).

The case of a single-slab waveguide with an imaginary gauge leads to two remarkable observations. First, the application of an imaginary vector potential perpendicular to the propagation direction does not alter the dispersion relation. In other words, the waveguide dispersion is equal to that of a conventional waveguide (see Supplemental Material [60]). Second, the mode profile in Fig. 1(a) has a pronounced asymmetry, which depends on the direction in which the gauge is being applied. In particular, the amplitude of the field at the left-hand side of the waveguide is different from that at the right-hand side. This is a highly interesting feature that will allow for the enhancement or suppression of optical forces when two gauge waveguides are brought together. In particular, the asymmetric profile may generate optical forces that cannot be excited in waveguides with macroscopic gain.

Let us now consider the effect of imaginary gauges on the solutions of two coupled waveguides, and in particular the optical forces between them. The optical force between two conventional dielectric slab waveguides at a distance $2b$ with core thickness a has been studied thoroughly in previous works [38]. In Figs. 1(c)–1(d), we obtain identical observations for evanescently coupled gauge waveguides: the modes of the isolated waveguides, characterized by black curves, hybridize. They split into even modes (blue dispersion curves) and odd modes (red dispersion curves) with respect to the symmetry plane at $x = 0$. Again, the imaginary vector potential does not influence the dispersion of the modes. To calculate the optical force acting on these waveguides, we make use of the Lorentz force and insert macroscopic fields (see Supplemental Material [60]). Importantly, the time-averaged total force $\langle \mathbf{F} \rangle$ on a volume V surrounded by the surface S contains not only the usual contributions due to the divergence of the Maxwell stress tensor $\langle \mathbf{T} \rangle$ and the time-derivative of Poynting's vector $\langle \epsilon_0 n^2 \mathbf{E} \times \mathbf{B} \rangle$. In addition to these contributions, we find a third term that determines the force acting on a waveguide:

$$\langle \mathbf{F} \rangle = \oint_S \langle \mathbf{T} \rangle \cdot d\mathbf{S} + \left\langle \int_V \epsilon_0 n^2 \frac{\partial}{\partial t} (\mathbf{E} \times \mathbf{B}) dV \right\rangle + \left\langle i\epsilon_0 \int_V \{ \tilde{\mathbf{A}} (n^2 |E|^2 + c^2 |B|^2) - 2[n^2 (\tilde{\mathbf{A}} \cdot \mathbf{E}) \mathbf{E} + c^2 (\tilde{\mathbf{A}} \cdot \mathbf{B}) \mathbf{B}] \} dV \right\rangle.$$

The additional term explicitly depends on the vector potential $\tilde{\mathbf{A}}$. In case of an imaginary vector potential $\tilde{\mathbf{A}} = i\,\tilde{A}\,\mathbf{1}_x$, the last term does not vanish and plays a major role in the enhancement and sign flip of the force. Therefore, the vector potential influences the optical force both in a direct way, through the explicit gauge-dependent terms, and in an indirect way, through a modification of the mode profiles. Real vector potentials do not enhance optical forces, because they do not appear in the Lorentz force and do not affect the symmetry of the mode profile. Further details regarding our method are provided in the Supplemental Material [60].

In Fig. 2, we visualize the dependence of the optical force on the strength of the imaginary gauge potential in the case of the fundamental transverse electric mode profile. The imaginary gauge potential is represented in terms of the accumulated amplification between both interfaces of the core $\Phi = a\tilde{A}$ (horizontal axis), which is defined in such a way that it is positive (negative) when the gauge potentials in both slabs point away from (towards) each

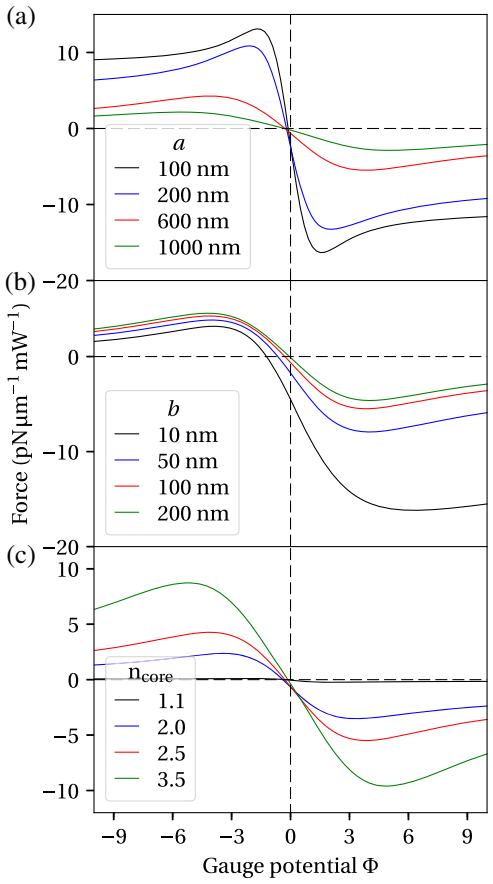

FIG. 2. Optical gradient force as a function of the applied gauge potential $\Phi = a\tilde{A}$ with gauge fields pointing away from (towards) each other $\Phi > 0$ ($\Phi < 0$) for different values of the waveguide thickness a, gap width $2b$, and core refractive index n_{core} at a wavelength of $\lambda = 1.55$ μm. (a) The forces increase for small waveguide thicknesses a with $2b = 200$ nm and $n_{\mathrm{core}} = 2.5$. (b) The forces increase for small gap widths $2 \cdot b$ with $a = 600$ nm, $n_{\mathrm{core}} = 2.5$, and (c) the forces increase for high refractive indices of the cores n_{core} with $a = 600$ and $2b = 200$ nm. The obtained values of the optical forces at zero gauge fields are in agreement with the current state-of-the-art results.

other. The different curves in Fig. 2 show how the force depends on the waveguide thickness a [Fig. 2(a)], the gap width $2b$ [Fig. 2(b)], and the refractive index of the core n_{core} [Fig. 2(c)]. For gauge potentials pointing away from each other, the attractive force due to the even mode is enhanced, while gauge potentials pointing towards each other counteract the attractive force. When the accumulated amplification Φ is sufficiently large, it is even possible to switch the sign of the force, from an attractive to a repulsive one. This is a novel feature that cannot be achieved by coupling conventional waveguides [38]: traditionally, mode profiles that are even (odd) with respect to the symmetry plane $x = 0$ cannot experience repulsive (attractive) forces.

In order to consistently compare optical forces that arise in waveguide pairs of different thickness and different gap width, the forces in Fig. 2 have been normalized with respect to the total power P_{in} that is coupled into the waveguides [32]. In a realistic setup, a pair of conventional waveguides would transport the guided mode to a pair of gauge waveguides and it is the power launched into the conventional waveguides that would be an experimentally available parameter. Therefore, we have normalized the optical forces between the waveguides in such a way that they correspond to a total incident power of 1 mW/μm inside the pair of conventional waveguides. The appropriate power that is transported by the mode profile of the gauge waveguides is subsequently calculated by making use of the overlap principle [66]. For more information on normalization, we refer to the Supplemental Material [60].

As shown in Fig. 2, variations in the applied gauge potential may lead to a tenfold enhancement of the optical force. Imaginary gauges require external energy input. It is thus important to compare our gauge waveguide implementation with gain waveguides. In the Supplemental Material, we show that for a fixed force enhancement our gauge waveguides are more energy efficient than traditional gain waveguides in an experimentally interesting parameter range, not only because of gain saturation, which ultimately limits the enhancement of gain waveguides, but also because of the more efficient distribution of the modal field profile in our setup [60]. Realistic values for Φ based on current realizations of gain-loss media with imaginary refractive indices of $n_i = 2$ enhance the force more than fourfold [67]. Of course, the aforementioned enhancements are also sensitive to the geometry of the system: thin waveguides with small gap widths and high refractive indices lead to stronger force enhancements. These geometrical dependencies also appear in coupled waveguides without gauges: small waveguide thicknesses result in weakly confined modes with high electric fields at the other waveguide. Note that, in the presence of a gauge, thin waveguides are more susceptible to force enhancement. For a particular value of the flux $\Phi = a\tilde{A}$, the amplitude of the imaginary vector potential increases and the gauge-dependent terms inside the optical force contribute more strongly to its enhancement. At fixed potentials Φ, forces will decrease or increase the gap width $2b$, depending on the sign of the force for the initial gap width $2b_0$, until the optical forces are compensated for by the elastic properties of the waveguides. More interesting dynamics is expected to occur when gauge potentials switch sign or change slowly in time.

In conclusion, we have shown that the application of complex-valued vector potentials perpendicular to the plane of coupled slab waveguides may enhance the force by an order of magnitude as compared to conventional waveguide systems. The mechanism behind this enhancement is twofold. On the one hand, complex-valued gauges introduce asymmetric mode profiles. Depending on the orientation of the vector potential, the electric field inside the gap and the associated optical forces may be enhanced or suppressed. On the other hand, the vector potential also explicitly introduces gauge-dependent terms into the expression of the optical force due to minimal substitution. The explicit dependence on the vector potential results in new features, such as switching from attractive to repulsive forces for even mode profiles. In addition to these new features, an implementation of complex-valued vector potentials in waveguides based on non-Hermitian coupled resonator lattices [59,61,62,65], as proposed in the Supplemental Material [60], would allow for a mechanism that is not susceptible to gain saturation. Given the recent interest in the generation of directional gain, we believe that complex-valued gauges provide a valuable new mechanism for the long-sought-after enhancement of optical forces in integrated switches and actuators.

V. G. and S. V. acknowledge fellowships from the Research Foundation Flanders (FWO-Vlaanderen). Work at VUB was partially supported by the Research Council of the VUB and by the Interuniversity Attraction Poles programme of the Belgian Science Policy Office, under Grant No. IAP P7-35.

*Vincent.Ginis@vub.ac.be

[1] P. W. Milonni and R. W. Boyd, Adv. Opt. Photonics **2**, 519 (2010).
[2] J. H. Poynting, Philos. Mag. **9**, 393 (1905).
[3] P. Lebedew, Ann. Phys. (Berlin) **311**, 433 (1901).
[4] E. F. Nichols and G. F. Hull, Phys. Rev. (Series I) **17**, 26 (1903).
[5] T. J. Kippenberg and K. J. Vahala, Science **321**, 1172 (2008).
[6] M. Aspelmeyer, T. J. Kippenberg, and F. Marquardt, Rev. Mod. Phys. **86**, 1391 (2014).
[7] J. Chen, J. Ng, Z. Lin, and C. T. Chan, Nat. Photonics **5**, 531 (2011).
[8] M. Padgett and R. Bowman, Nat. Photonics **5**, 343 (2011).
[9] D. G. Grier, Nature (London) **424**, 810 (2003).
[10] K. Y. Bliokh, A. Y. Bekshaev, and F. Nori, Nat. Commun. **5**, 3300 (2014).

[11] S. B. Wang and C. T. Chan, Nat. Commun. **5**, 3307 (2014).
[12] F. J. Rodríguez-Fortuño, N. Engheta, A. Martínez, and A. V. Zayats, Nat. Commun. **6**, 8799 (2015).
[13] A. Ashkin, Phys. Rev. Lett. **24**, 156 (1970).
[14] L. Tong, V. D. Miljkovic, and M. Käll, Nano Lett. **10**, 268 (2010).
[15] O. M. Maragò, P. H. Jones, P. G. Gucciardi, G. Volpe, and A. C. Ferrari, Nat. Nanotechnol. **8**, 807 (2013).
[16] V. Kajorndejnukul, W. Ding, S. Sukhov, C. Qiu, and A. Dogariu, Nat. Photonics **7**, 787 (2013).
[17] V. Shvedov, A. R. Davoyan, C. Hnatovsky, N. Engheta, and W. Krolikowski, Nat. Photonics **8**, 846 (2014).
[18] L. Liu, S. Kheifets, V. Ginis, and F. Capasso, Phys. Rev. Lett. **116**, 228001 (2016).
[19] A. Ashkin and J. P. Gordon, Opt. Lett. **4**, 161 (1979).
[20] C. N. Cohen-Tannoudji, Rev. Mod. Phys. **70**, 707 (1998).
[21] M. P. MacDonald, G. C. Spalding, and K. Dholakia, Nature (London) **426**, 421 (2003).
[22] A. Jonáš and P. Zemanek, Electrophoresis **29**, 4813 (2008).
[23] M. Zhong, X. Wei, J. Zhou, Z. Wang, and Y. Li, Nat. Commun. **4**, 1768 (2013).
[24] P. Galajda and P. Ormos, Appl. Phys. Lett. **78**, 249 (2001).
[25] M. Liu, T. Zentgraf, Y. Liu, G. Bartal, and X. Zhang, Nat. Nanotechnol. **5**, 570 (2010).
[26] D. Van Thourhout and J. Roels, Nat. Photonics **4**, 211 (2010).
[27] H. Cai, B. Dong, J. F. Tao, L. Ding, J. M. Tsai, G. Lo, A. Q. Liu, and D. L. Kwong, Appl. Phys. Lett. **102**, 023103 (2013).
[28] P. Zhang, N. Shen, T. Koschny, and C. M. Soukoulis, ACS Photonics **4**, 181 (2017).
[29] M. L. Povinelli, M. Ibanescu, S. G. Johnson, and J. D. Joannopoulos, Appl. Phys. Lett. **85**, 1466 (2004).
[30] A. Xuereb, C. Genes, and A. Dantan, Phys. Rev. Lett. **109**, 223601 (2012).
[31] A. Xuereb, C. Genes, and A. Dantan, Phys. Rev. A **88**, 053803 (2013).
[32] V. Ginis, P. Tassin, C. M. Soukoulis, and I. Veretennicoff, Phys. Rev. Lett. **110**, 057401 (2013).
[33] M. Righini, A. S. Zelenina, C. Girard, and R. Quidant, Nat. Phys. **3**, 477 (2007).
[34] A. N. Grigorenko, N. W. Roberts, M. R. Dickinson, and Y. Zhang, Nat. Photonics **2**, 365 (2008).
[35] M. Li, W. H. P. Pernice, C. Xiong, T. Baehr-Jones, M. Hochberg, and H. X. Tang, Nature (London) **456**, 480 (2008).
[36] G. S. Wiederhecker, L. Chen, A. Gondarenko, and M. Lipson, Nature (London) **462**, 633 (2009).
[37] J. Zhang, K. F. MacDonald, and N. I. Zheludev, Phys. Rev. B **85**, 205123 (2012).
[38] M. L. Povinelli, M. Lončar, M. Ibanescu, E. J. Smythe, S. G. Johnson, F. Capasso, and J. D. Joannopoulos, Opt. Lett. **30**, 3042 (2005).
[39] V. Liu, M. Povinelli, and S. Fan, Opt. Express **17**, 21897 (2009).
[40] J. J. Xiao, J. Ng, Z. Lin, and C. T. Chan, Appl. Phys. Lett. **94**, 011102 (2009).
[41] R. Van Laer, B. Kuyken, D. Van Thourhout, and R. Baets, Nat. Photonics **9**, 199 (2015).
[42] J. D. Jackson, *Classical Electrodynamics* (John Wiley & Sons, New York, 2007).
[43] F. Bloch, Z. Phys. **52**, 555 (1929).
[44] Y. Aharonov and D. Bohm, Phys. Rev. **115**, 485 (1959).
[45] M. Z. Hasan and C. L. Kane, Rev. Mod. Phys. **82**, 3045 (2010).
[46] D. Jaksch and P. Zoller, New J. Phys. **5**, 56 (2003).
[47] Z. Wang, Y. Chong, J. Joannopoulos, and M. Soljačić, Nature (London) **461**, 772 (2009).
[48] Y. Lin, R. L. Compton, K. Jiménez-García, W. D. Phillips, J. V. Porto, and I. B. Spielman, Nat. Phys. **7**, 531 (2011).
[49] K. Jimenez-Garcia, L. J. LeBlanc, R. A. Williams, M. C. Beeler, A. R. Perry, and I. B. Spielman, Phys. Rev. Lett. **108**, 225303 (2012).
[50] M. Hafezi, S. Mittal, J. Fan, A. Migdall, and J. M. Taylor, Nat. Photonics **7**, 1001 (2013).
[51] A. B. Khanikaev, S. Hossein Mousavi, W. Tse, M. Kargarian, A. H. MacDonald, and G. Shvets, Nat. Mater. **12**, 233 (2013).
[52] L. Lu, J. D. Joannopoulos, and M. Soljacic, Nat. Photonics **8**, 821 (2014).
[53] L. D. Tzuang, K. Fang, P. Nussenzveig, S. Fan, and M. Lipson, Nat. Photonics **8**, 701 (2014).
[54] F. Liu, S. Wang, S. Xiao, Z. H. Hang, and J. Li, Appl. Phys. Lett. **107**, 241106 (2015).
[55] F. Liu and J. Li, Phys. Rev. Lett. **114**, 103902 (2015).
[56] Q. Lin and S. Fan, Phys. Rev. X **4**, 031031 (2014).
[57] Y. Plotnik, M. A. Bandres, S. Stützer, Y. Lumer, M. C. Rechtsman, A. Szameit, and M. Segev, Phys. Rev. B **94**, 020301 (2016).
[58] Y. Lumer, M. A. Banders, H. H. Sheinfux, Y. Plotnik, M. Heinrich, A. Szameit, and M. Segev, 2016 Conference on Lasers and Electro-Optics (CLEO) (Optical Society of America, 2016), Vol. 1, paper FM3A.3, https://doi.org/10.1364/CLEO_QELS.2016.FM3A.3.
[59] S. Longhi, D. Gatti, and G. Della Valle, Sci. Rep. **5**, 13376 (2015).
[60] See Supplemental Material at http://link.aps.org/supplemental/10.1103/PhysRevLett.119.137402 providing a detailed calculation of the mode profile in the presence of an effective vector potential, of the optical forces between coupled gauge waveguides and of the energy cost of gauge waveguides as compared to gain waveguides.
[61] Y. Hadad and B. Z. Steinberg, Phys. Rev. Lett. **105**, 233904 (2010).
[62] H. Ramezani, T. Kottos, R. El-Ganainy, and D. N. Christodoulides, Phys. Rev. A **82**, 043803 (2010).
[63] R. O. Umucalılar and I. Carusotto, Phys. Rev. A **84**, 043804 (2011).
[64] K. Fang, Z. Yu, and S. Fan, Nat. Photonics **6**, 782 (2012).
[65] A. Regensburger, C. Bersch, M. Miri, G. Onishchukov, D. N. Christodoulides, and U. Peschel, Nature (London) **488**, 167 (2012).
[66] R. R. A. Syms and J. Cozens, *Optical Guided Waves and Devices* (McGraw-Hill, New York, 1992).
[67] O. Hess, J. B. Pendry, S. A. Maier, R. F. Oulton, J. M. Hamm, and K. L. Tsakmakidis, Nat. Mater. **11**, 573 (2012).